

Correlation between weak ferromagnetism and crystal symmetry in Gd_2CuO_4 -type cuprates

H. M. Luo, Y. Y. Hsu, B. N. Lin, Y. P. Chi, T. J. Lee, and H. C. Ku

Department of Physics, National Tsing Hua University, Hsinchu 300, Taiwan

(Received 8 January 1999)

Correlation between copper weak ferromagnetism (WF) and crystal structural symmetry of the $Gd_{2-x}M_xCuO_4$ ($M=Bi$ or Tb ; $0 \leq x \leq 0.5$) systems is reported. Detailed powder x-ray Rietveld refinement analysis on $Gd_{2-x}M_xCuO_4$ shows a systematic variation of oxygen distortion angle $\alpha(\text{Cu-O-Cu})$ with ionic size where the lattice layer mismatch lowers the crystal symmetry to an orthorhombic O' -phase with pseudo-tetragonal lattice parameter $a_0 \sim b_0 \sim 5.508 \text{ \AA}$. Weak ferromagnetic or canted antiferromagnetic order is the direct result of this oxygen distortion which causes a σ -transfer $\text{Cu}(3d_{x^2-y^2})\text{-O}(2p_\sigma)\text{-Cu}(3d_{x^2-y^2})$ superexchange interaction in the CuO_2 plane with a non- 180° coupling angle. The small WF saturation moment m_s of $\sim 2-6 \times 10^{-2} \mu_B/\text{Cu}^{2+}$ can be deduced from the copper moment $\mu(\text{Cu}^{2+})$ canting angle $\theta = (\pi - \alpha)/2 \sim 2-7^\circ$. Magnetic data and internal exchange field B_{int} estimation indicate that Cu^{2+} WF saturation moment $m_s(\text{Cu}^{2+})$ decreases with larger Bi^{3+} doping and increases with smaller Tb^{3+} doping. [S0163-1829(99)03341-X]

I. INTRODUCTION

For the high- T_c cuprate systems, superconductivity always occurs near the metal-insulator transition boundary due to strong electron correlation. In the insulator side, copper magnetic moment $\mu(\text{Cu}^{2+})$ (d^9 , $s = \frac{1}{2}$) forms a three-dimensional (3D) long-range magnetic ordering through the quasi-2D σ -transfer $\text{Cu}(3d_{x^2-y^2})\text{-O}(2p_\sigma)\text{-Cu}(3d_{x^2-y^2})$ indirect superexchange interaction in the CuO_2 layers. It is observed that Cu spins in most cuprate insulators form an antiparallel antiferromagnetic (AF) arrangement below Néel temperature $T_N(\text{Cu})$ with zero saturation moment $m_s(\text{Cu}^{2+})$. However, a peculiar Cu weak ferromagnetic (WF) or canted antiferromagnetic (CAF) order with nonzero m_s is observed below $T_N(\text{Cu}) \sim 260\text{--}285 \text{ K}$ for the tetragonal T' -phase Gd_2CuO_4 ,¹⁻¹⁵ and a true AF order is recovered only at a much lower temperature of $T_{\text{sr}}(\text{Cu}) \sim 20 \text{ K}$ through spin reorientation. At temperature around $7\text{--}8 \text{ K}$, a possible 3D to quasi-2D crossover for Cu AF ordering is reported from neutron study before the Gd^{3+} sublattice AF ordering of $T_N(\text{Gd}) \sim 6.5\text{--}7 \text{ K}$.¹⁵ At even lower temperature, a heat capacity broad shoulder followed with a peak near 2 K is observed,⁸ indicating complex magnetic phase diagram at low temperature due to Gd-Cu interaction.

Extensive magnetic and structural studies on Gd_2CuO_4 (Refs. 1-15) and related compounds $(Gd,M)_2CuO_4$ ($M=R^{3+}$ rare earths, Ce^{4+} , Si^{2+} , or Bi^{3+}),^{3-5,7-10,14} and metastable systems R_2CuO_4 ($R=Y, \text{Tb-Tm}$) and related compounds¹⁶⁻²¹ are reported. Since the occurrence of weak ferromagnetism requires an additional antisymmetric Dzyaloshinsky-Moriya-type exchange interaction term in otherwise symmetric Cu-O-Cu superexchange interaction, it is speculated that a slight oxygen distortion in the CuO_2 layer is necessary for Cu WF/CAF order in the Gd_2CuO_4 -type cuprates.^{2,5-14} Although single-crystal x-ray diffraction on Gd_2CuO_4 gives a good fitting using the tetragonal T' -phase space group $14/mmm$ with Cu(0,0,0) and oxygen O(1)($0, \frac{1}{2}, 0$) in CuO_2 layer formed a perfect square-planar arrangement,¹

large plane oxygen mean-square displacement U_{eq} of 2.5 \AA^2 at room temperature indicates that stable oxygen position may not be in the ideal $(0, \frac{1}{2}, 0)$ sites. Single-crystal neutron diffraction of $^{158}\text{Gd}_2\text{CuO}_4$ based on T' -phase structure shows that Cu moments order below $T_N(\text{Cu})$ to a basically AF structure with the propagation vector $\mathbf{k} = (\frac{1}{2}, \frac{1}{2}, 0)$ and the Cu moments are oriented parallel to the $[110]$ direction of the tetragonal basal plane.^{6,8} The inconsistency between weak ferromagnetism and x-ray/neutron-diffraction data indicates that a distorted T' structure is necessary to account for the WF/CAF order. Recently, a neutron structural study at room temperature reports a long-range superstructure of the T' phase in Gd_2CuO_4 . The oxygen squares surrounding the Cu sites are found to rotate around the c axis by a small angle ($\sim 5^\circ$) which leads to a reduced orthorhombic symmetry (space group Acam).¹² This structural deformation from T' phase to O' phase is believed to be crucial for the occurrence of weak ferromagnetism.

In order to study the correlation between Cu weak ferromagnetism and crystal symmetry, we report here a detailed magnetic and powder x-ray Rietveld structural studies on Gd_2CuO_4 and related systems $(Gd,M)_2CuO_4$ ($M=Bi$ or Tb).

II. EXPERIMENTS

The $Gd_{2-x}Bi_xCuO_{4+\delta}$ ($0 \leq x \leq 0.1$) and $Gd_{2-x}Tb_xCuO_{4+\delta}$ ($0 \leq x \leq 0.5$) samples with nominal composition were synthesized by solid-state reaction using high-purity Gd_2O_3 (99.99%), Bi_2O_3 (99.999%), Tb_4O_7 (99.9%) and CuO (99.9%) powders. Samples were thoroughly mixed and carefully calcined between $900\text{--}950^\circ\text{C}$ in air for 1 day with several intermediate regrindings. The calcined powders were then pressed into pellets and sintered in air at 1000°C for 2 days and air quenched to room temperature. Oxygen content parameter δ was determined from the standard iodometric titration method to be < 0.003 .

Powder x-ray Rietveld analysis data were obtained with a Rigaku Rotaflex 18-kW rotating anode diffractometer using

TABLE I. Structural parameters of orthorhombic O' phase Gd_2CuO_4 .

Formula	Gd_2CuO_4					
Temperature	300 K					
Space group	$Acam$ ($Cmca$, No. 64) $Z=4$					
Cell parameters	$a=5.5082(5)$ Å, $b=5.5084(5)$ Å, $c=11.8864(10)$ Å, $V=360.65(3)$ Å ³					
Radiation λ (Å)	Cu- $K_{\alpha 1}$ (1.540 60), Cu- $K_{\alpha 2}$ (1.544 43)					
Diffractometer	Rigaku Rotaflex 18-kW rotating anode					
Measurement range, 2θ	20–100°					
Step size, 2θ	0.02°					
Atom	Position	x	y	z	Occupancy	B_{iso} (Å ²)
Gd	8d	0	0	0.3495	1	0.34
Cu	4a	0	0	0	1	0.54
O(1)	8f	0.2719	0.2240	0	1	0.77
O(2)	8e	1/4	0.2513	1/4	1	0.71
R factors: $R_p=6.99\%$, $R_{wp}=7.07\%$, $R_B=7.00\%$ (209 reflections)						
Selected interatomic distances (Å) and angle (degree)						
Cu-Cu	3.895			Cu-O(1)-Cu	169.1°	
Cu-O(1)	1.941	1.972				
Cu-O(2)	3.550	3.556				
Gd-Gd	3.578					
Gd-O(1)	2.510	2.639				
Gd-O(2)	2.274	2.283				

graphite monochromatized Cu- K_{α} radiation with a scanning step of 0.02° (10-second counting time per step) in the 2θ range of 20–100°. A RIQAS refinement program²² was used with inorganic crystal structure database (ICSD) and diffraction database (ICDD). The magnetization and magnetic susceptibility measurements were carried out with a Quantum Design MPMS or a μ -metal shielded MPMS₂ superconducting quantum interference device (SQUID) magnetometer down to 2 K in applied magnetic fields from 1 G–5 T.

III. RESULTS AND DISCUSSION

In the R_2CuO_4 insulating system ($R=Pr, Nd, Sm, Eu, Gd$), Gd_2CuO_4 compound with the smallest Gd^{3+} ionic radius²³ of 0.938 Å is the only member which shows weak ferromagnetism. If the oxygen distortion in the CuO_2 layer is crucial for the formation of this peculiar WF/CAF order, then the cause of oxygen distortion must be closely related with the lattice layer mismatch between smaller $(Gd-O)_2$ layers and CuO_2 layer. Since all other R_2CuO_4 compounds with larger rare earth R^{3+} ions show no sign of WF order, a doping in the Gd sites with larger non-rare-earth Bi^{3+} ions (0.96 Å) should also reduce the degree of oxygen distortion in the CuO_2 layer.

In order to study the correlation between weak ferromagnetism and oxygen distortion, powder x-ray Rietveld structural refinement analysis was performed on the Bi^{3+} -doped compounds $Gd_{2-x}Bi_xCuO_{4+\delta}$ ($x=0, 0.05, \text{ and } 0.07$) at room temperature. Very small oxygen content parameter δ of <0.003 determined from iodometric titration can be ne-

glected. Based on the previous reported orthorhombic space group $Acam$ ($Cmca$) from neutron study with fully occupied atomic positions,¹² the scale factor, lattice parameters, atom coordinates, and isotropic temperature factors were refined. For the undoped Gd_2CuO_4 sample, the final step-pattern R factor R_p of 6.99% and weighted-pattern R_{wp} of 7.07% were obtained with goodness-of-fit parameter s of 2.82 for 4001 steps. The Bragg reflection R factor R_B was 7.00% for 209 reflections. The structural parameters for the orthorhombic O' -phase Gd_2CuO_4 are listed in Table I and the refinement patterns are shown in Fig. 1. Good fitting between the calcu-

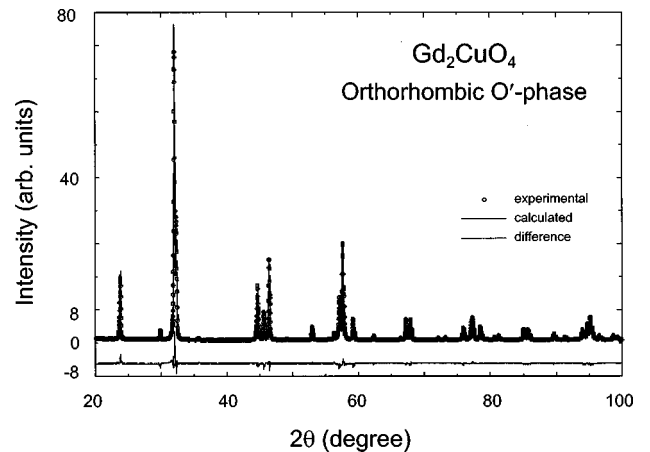


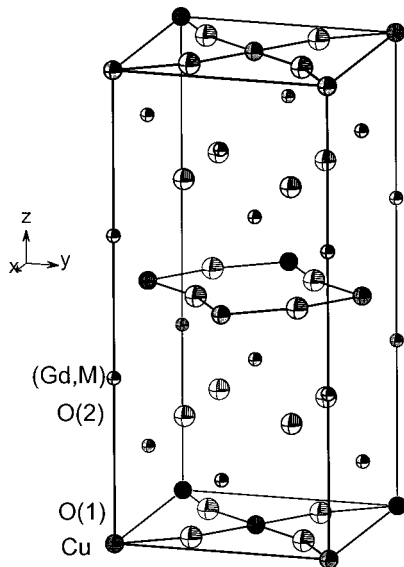
FIG. 1. Experimental (dotted), calculated (curve) and difference of the powder x-ray-diffraction patterns of orthorhombic O' phase Gd_2CuO_4 at room temperature.

TABLE II. Structural parameters of undistorted tetragonal T' -phase model for Gd_2CuO_4 .

Formula		Gd_2CuO_4					
Space group		$I4/mmm$ (No. 139)		$Z=2$			
Cell parameters		$a=3.8953(3) \text{ \AA}$,		$c=11.8864(10) \text{ \AA}$			
Atom	Position	x	y	z	Occupancy	$B_{iso} (\text{Å}^2)$	
Gd	$4e$	0	0	0.3495	1	0.34	
Cu	$2a$	0	0	0	1	0.54	
O(1)	$4c$	0	1/2	0	1	1.70	
O(2)	$4d$	0	1/2	1/4	1	0.71	

R factors: $R_p=8.13\%$, $R_{wp}=7.09\%$, $R_B=7.60\%$ (84 reflections)
 Selected interatomic distances (Å) and angle (degree)
 Cu-Cu 3.895 Cu-O(1)-Cu 180°
 Cu-O(1) 1.948

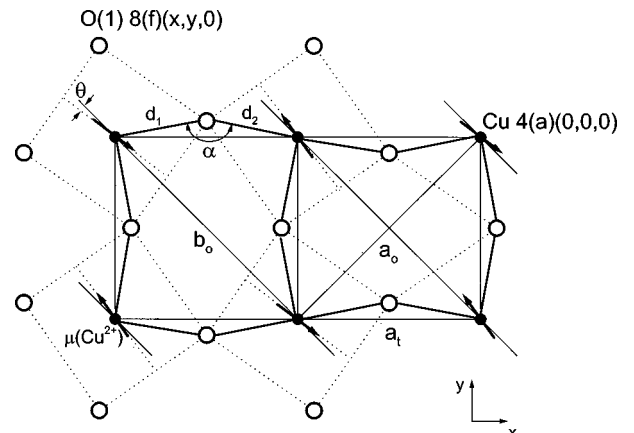
lated and experimental patterns shows the success of the orthorhombic model. Note that almost identical orthorhombic lattice parameters $a_0=5.5082 \text{ \AA} \sim b_0=5.5084 \text{ \AA}$ indicate that this high-temperature O' phase (HTO') is highly pseudotetragonal. However, using the original tetragonal T' -phase model with space group $I4/mmm$ and lattice parameter $a_t=3.8953 \text{ \AA} \sim a_0/\sqrt{2}$, a very large isotropic temperature factor B_{iso} or mean-square displacement of 1.7 \AA^2 for plane oxygen O(1) in the ideal $(0, \frac{1}{2}, 0)$ sites is deduced (see Table II, with larger $R_p=8.13\%$, $R_{wp}=7.09\%$, and $R_B=7.60\%$), indicates that oxygens in the CuO_2 plane are not likely to be located in this undistorted positions at room temperature. On the other hand, using the slightly distorted O(1)(0.272,0.224,0) sites of the orthorhombic space group $Acam$, B_{iso} reduces dramatically to 0.77 \AA^2 , shows that even with pseudotetragonal structure, an oxygen distortion from the ideal tetragonal sites is necessary to obtain better structural refinement. This formation of high-temperature O' phase is believed to be crucial for the occurrence of copper

Orthorhombic O' -phaseFIG. 2. Crystal structure of orthorhombic O' phase $(Gd,M)_2CuO_4$ cuprates.

weak ferromagnetism. Similar results were obtained for the Bi-doped compounds.

Figure 2 shows the schematic representation of orthorhombic O' phase of $(Gd,M)_2CuO_4$ cuprates ($M=Bi, Tb$). The O' phase is very similar to the body-centered-tetragonal T' phase except for slight oxygen distortion in the CuO_2 plane with no apical oxygen. The oxygen distortion is believed to be caused by the lattice layer mismatch between the smaller $[(Gd,M)-O]_2$ layers and CuO_2 plane.

The proposed correlation between weak ferromagnetic/canted antiferromagnetic (WF/CAF) order and structural symmetry in the CuO_2 plane for temperature range $T_{sr}(Cu) < T \leq T_N(Cu) < 300 \text{ K}$ is shown in Fig. 3.^{6,12} The CuO_2 plane of the HTO' phase is no longer a perfect square plane. The rotation/displacement of the O(1) $8(f)(x,y,0)$ squares around the Cu sites leads to two unequal Cu-O(1) bond lengths of $d_1=1.941 \text{ \AA}$ and $d_2=1.972 \text{ \AA}$ for Gd_2CuO_4 and a Cu-O(1)-Cu bond angle α of 169.1° instead of 180° . Since the Cu- $3d_{x^2-y^2}$ orbital is anisotropic, in order to achieve maximum wave-function overlap with nonorthogonal AF coupling between Cu- $3d_{x^2-y^2}$ and O- $2p_\sigma$ orbitals, the Cu orbital and thus its magnetic moment $\mu(Cu^{2+})$ must cant a small angle $\theta=(\pi-\alpha)/2$ of 5.4° away from the orthorhombic $[100]/[010]$ direction or the pseudotetragonal $[110]$ direc-

FIG. 3. The proposed Cu^{2+} weak ferromagnetic/canted antiferromagnetic (WF/CAF) structure in the CuO_2 plane at $T_{sr}(Cu) < T \leq T_N(Cu)$ for the orthorhombic Gd_2CuO_4 -type cuprates.

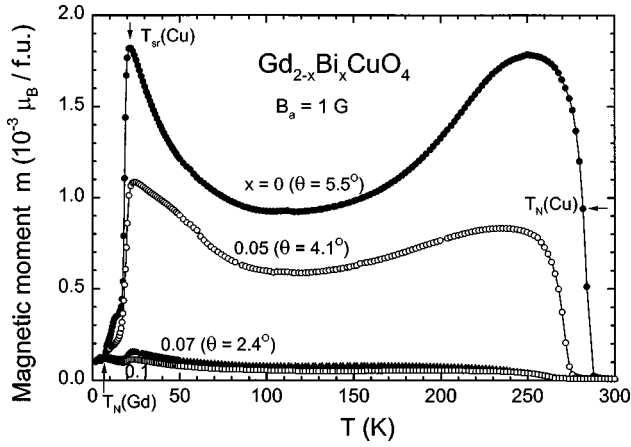


FIG. 4. Temperature dependence of magnetized magnetic moment per formula unit $m(T)$ with estimated magnetic canting angle θ for larger Bi^{3+} -doped $\text{Gd}_{2-x}\text{Bi}_x\text{CuO}_4$ ($x=0, 0.05, 0.07,$ and 0.1) polycrystalline bulk samples in a low applied field B_a of 1 G.

tion observed from preliminary low-temperature neutron data.⁶ This creates an additional antisymmetric Dzyaloshinsky-Moriya-type exchange interaction term and the effective interaction between Cu spins in the CuO_2 plane is still the 2D σ -transfer type but with an angle $\alpha(\text{Cu-O(1)-Cu}) \neq 180^\circ$. Below 3D ordering temperature $T_N(\text{Cu})$ of 282 K, the canted antiferromagnetic (CAF) alignment will create a net WF saturation moment $m_s(\text{Cu}^{2+}) = \mu(\text{Cu}^{2+}) \cdot \sin \theta$. If the usual neutron-derived copper moment of $\mu(\text{Cu}^{2+}) \sim 0.3-0.5 \mu_B$ is used,²⁴ then the saturation moment m_s of $\sim 3-5 \times 10^{-2} \mu_B / \text{Cu}^{2+}$ is derived using room temperature canting angle θ of 5.45° .

If the WF saturation moment m_s is closely related to the Cu-O(1)-Cu bonding angle α , a systematic variation of WF order can then be deduced for the Bi-doped system through the Rietveld refinement studies. The temperature dependence of low-field magnetization with estimated magnetic moment canting angle θ for the Bi-doped $\text{Gd}_{2-x}\text{Bi}_x\text{CuO}_4$ ($x=0, 0.05, 0.07,$ and 0.1) (Ref. 14) polycrystalline bulk samples with solubility limit of $x \leq 0.1$ is shown in Fig. 4. A monotonical decrease of magnetized magnetic moment per formula unit $m(T)$ and canting angle θ with progressive larger Bi^{3+} ion

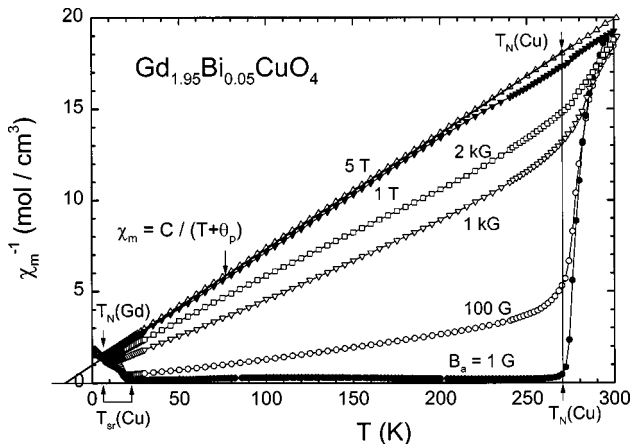


FIG. 5. Inverse molar magnetic susceptibility $\chi_m^{-1}(T)$ for $\text{Gd}_{1.95}\text{Bi}_{0.05}\text{CuO}_4$ in various applied fields of 1 G, 100 G, 1 kG, 2 kG, 1 T, and 5 T. The solid line is a Curie-Weiss fit with negative intercept θ_p .

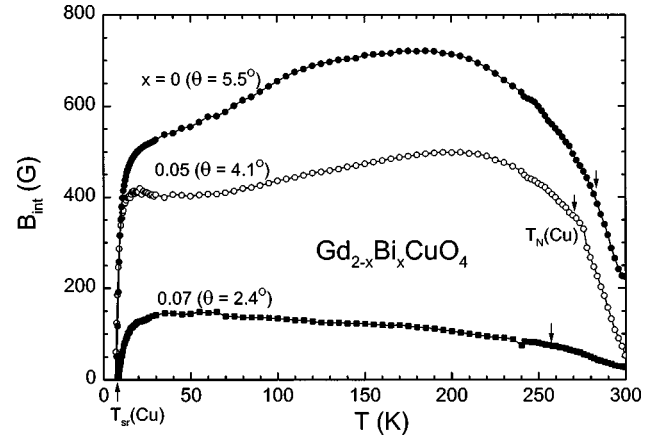


FIG. 6. Estimated WF internal exchange field $B_{\text{int}}(T)$ with estimated magnetic canting angle θ of the $\text{Gd}_{2-x}\text{Bi}_x\text{CuO}_4$ system ($x=0, 0.05,$ and 0.07) from high-field ($B_a > B_{\text{int}}$) magnetic data.

doping can be clearly seen. The low field of 1 G is used in order to minimize the interference from large Gd^{3+} moment $\mu(\text{Gd}^{3+})$ of $7 \mu_B$. With room-temperature paramagnetic magnetization m (300 K) of only $\sim 2 \times 10^{-5} \mu_B$ per formula unit in 1 G large magnetized moment of $\sim 1-2 \times 10^{-3} \mu_B / \text{f.u.}$ below $T_N(\text{Cu})$ is mostly from the magnetized WF domain with nonzero copper saturation moment $m_s(\text{Cu}^{2+})$ in each domain. $T_N(\text{Cu})$ decreases from 282 K for $x=0$ to 270 K for $x=0.05$, 258 K for $x=0.07$, and 256 K for $x=0.1$. The sharp decrease of magnetized moment below $T_{sr}(\text{Cu})$ around 22–24 K in 1 G indicates a Cu moment spin reorientation to the true AF ground state with zero saturation moment m_s . The Gd^{3+} moments eventually order antiferromagnetically at $T_N(\text{Gd})$ of 7 K for $x=0$ and 6.4 K for $x=0.1$.¹⁴

The copper WF/CAF saturation moment $m_s(\text{Cu}^{2+})$ is difficult to be determined directly from high-field magnetization measurements even with a well oriented single crystal due to the interference of large Gd^{3+} moment $\mu(\text{Gd}^{3+})$ and the nature of copper weak ferromagnetism, where the WF saturation moment m_s is always smaller than the copper moment $\mu(\text{Cu}^{2+})$ of $\sim 0.3-0.5 \mu_B$.²⁴ However, one can estimate the WF internal exchange field B_{int} created by the saturation moment m_s . For this purpose, inverse molar magnetic suscep-

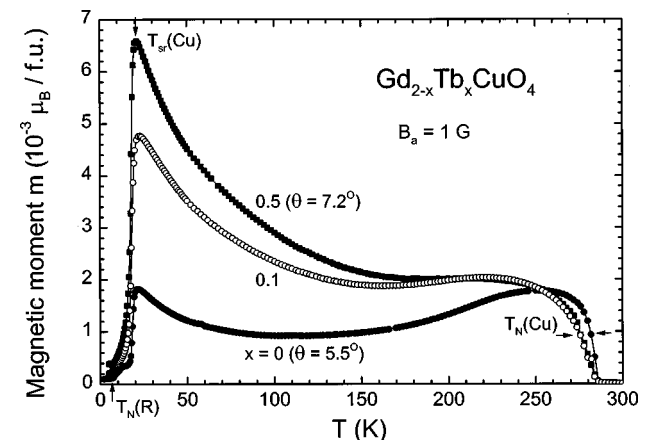


FIG. 7. Temperature dependence of magnetized magnetic moment $m(T)$ with estimated magnetic canting angle θ for smaller Tb^{3+} -doped $\text{Gd}_{2-x}\text{Tb}_x\text{CuO}_4$ system ($x=0, 0.1,$ and 0.5) in 1 G.

TABLE III. Magnetic and structural data of Bi-doped $\text{Gd}_{2-x}\text{Bi}_x\text{CuO}_4$ cupates. $T_N(\text{Cu})$: Cu WF/CAF order temperature; $T_{\text{sr}}(\text{Cu})$: Cu spin-reorientation temperatures at 2 kG and 1 G; B_{int} : maximum internal exchange field; a_0/b_0 : orthorhombic lattice parameters at room temperature; α : Cu-O(1)-Cu bond angle; $\theta = (\pi - \alpha)/2$: Cu spin canting angle; $m_s = \mu(\text{Cu}^{2+}) \cdot \sin \theta$: WF saturation moment.

x	$T_N(\text{Cu})$ (K)	$T_{\text{sr}}(\text{Cu})$ (K)	B_{int} (G)	a_0 (Å)	b_0 (Å)	α (°)	θ (°)	$m_s(\mu_B)$
0	282	9.5, 22	720	5.5082	5.5084	169.1	5.5	0.048
0.05	270	8.5, 24	500	5.5090	5.5092	171.8	4.1	0.036
0.07	258	~7, 24	150	5.5096	5.5097	175.2	2.4	0.021

tibilities $\chi_m^{-1}(T)$ for a typical Bi-doped $\text{Gd}_{1.95}\text{Bi}_{0.05}\text{CuO}_4$ compound in various applied fields B_a from 1 G–5 T are shown collectively in Fig. 5. $T_N(\text{Cu})$ of 270 K and $T_N(\text{Gd})$ of 6.5 K are nearly field independent. $T_{\text{sr}}(\text{Cu})$ decreases from 24 K in 1 G to 20 K in 100 G, 12 K in 1 kG, 8.5 K in 2 kG, ~7 K in 1 T, and merges with $T_N(\text{Gd})$ in 5 T. Since the weak internal field is only in the order of 10^2 – 10^3 G,³ the paramagnetic Gd^{3+} moment contribution increases its domination such that the magnetic susceptibility, in higher field can be approximately fitted with in a Curie-Weiss form of $\chi_m = C/(T + \theta_p)$. For $B_a = 5$ T, the Curie constant of $15.9 \text{ cm}^3 \text{ K/mol}$ gives an effective Gd^{3+} moment μ_{eff} of $7.99\mu_B$, which is close to the free ion $\mu_{\text{eff}}(\text{Gd}^{3+})$ of $7.94\mu_B$ if the small Cu^{2+} ordered moment is neglected. The negative Curie-Weiss intercept θ_p of 17.8 K is larger than $T_N(\text{Gd})/T_{\text{sr}}(\text{Cu})$ of ~6.6 K. The temperature dependence of the internal exchange field $B_{\text{int}}(T)$ for $T > T_{\text{sr}}(\text{Cu})$ can then be estimated using the formula³

$$B_{\text{int}}(T) \sim [M(T, B_a)/\chi_m(T)] - B_a,$$

where magnetization $M(T, B_a)$ is measured in an applied field $B_a \sim 1$ – $2 \text{ kG} > B_{\text{int}}$ and the Curie-Weiss susceptibility $\chi_m = C/(T + \theta_p)$ from higher field (~1–5 T) fitting is used. The estimated WF internal field B_{int} for the $\text{Gd}_{2-x}\text{Bi}_x\text{CuO}_4$ system ($x=0, 0.05, 0.07$) with estimated magnetic moment canting angle θ is shown in Fig. 6. The internal field is temperature dependent where maximum B_{int} observed decreases from around 720 G for $x=0$, to 500 G for $x=0.05$ and 150 G for $x=0.07$. For $T \sim T_{\text{sr}}(\text{Cu}) \sim 10$ K at B_a of 1–2 kG, B_{int} decreases sharply to zero due to the disappearance of copper saturation moment in the true AF state. Residual B_{int} observed above $T_N(\text{Cu})$ may be due to the simplified formula used or from the intrinsic 2D short-range quantum spin fluctuation.⁷ The small internal field of 720 G observed for Gd_2CuO_4 is consistent with this small saturation moment m_s . Since the structural-related canting angle $\theta(T)$ is temperature dependent, the saturation moment $m_s(T)$ in each WF domain wall and the internal exchange field $B_{\text{int}}(T)$ will also be temperature dependent. For temperature below $T_{\text{sr}}(\text{Cu})$, a WF/CAF to AF magnetic transition should be accompanied with an orthorhombic to tetragonal (or high-temperature HTO' phase to low-temperature LTT' phase) structural transition with $\theta=0$ in the true AF state. A detailed low-temperature magnetic and structural study is necessary to confirm this speculation. Table III shows the correlation between the magnetic and structural variation for the $\text{Gd}_{2-x}\text{Bi}_x\text{CuO}_4$ system. With slightly larger Bi doping ($r_{\text{Bi}^{3+}} = 0.96 \text{ Å} > r_{\text{Gd}^{3+}} = 0.938 \text{ Å}$), the orthorhombic lattice parameter a_0 and b_0 increase monotonically with progres-

sive Bi doping as expected. The unit-cell volume $V = a_0 b_0 c_0$ increases from 360.7 Å^3 for $x=0$ to 361.2 Å^3 for $x=0.07$. The longer Cu-O(1) bond lengths d_1 and d_2 during Bi doping decrease wave-function overlap and $T_N(\text{Cu})$ from 282 K for $x=0$ to 258 K for $x=0.07$. However, with large Bi doping, the lattice layer mismatch between the smaller $[(\text{Gd}, \text{Bi})\text{-O}]_2$ layers and CuO_2 plane is reduced, which results a less oxygen distortion in the CuO_2 plane. Smaller oxygen distortion restores the Cu-O(1)-Cu bond angle α from 169.1° for $x=0$ to 175.2° for $x=0.07$. The resulting smaller canting angle $\theta = (\pi - \alpha)/2$ of 2.4° for $x=0.07$ as compared with 5.5° for $x=0$ reduces the estimated copper WF saturation moment m_s from $4.8 \times 10^{-2} \mu_B$ to $2.1 \times 10^{-2} \mu_B$ using $\mu(\text{Cu}^{2+}) \sim 0.5 \mu_B$,²⁴ and the maximum internal field $B_{\text{int}}(\text{max})$ from 720–150 G.

Since Gd_2CuO_4 is the smallest stable compound in the $R_2\text{CuO}_4$ system under ambient pressure sample preparation condition, based on the similar ionic size consideration, a doping in the Gd sites with smaller rare-earth R^{3+} ions should increase the oxygen distortion in the CuO_2 layer. The temperature dependence of magnetization for smaller Tb^{3+} -doped system $\text{Gd}_{2-x}\text{Tb}_x\text{CuO}_4$ ($x=0, 0.1, \text{ and } 0.5$) is shown in Fig. 7. A monotonical increase of magnetized magnetic moment per formula unit $m(T)$ as well as canting angle θ with progressive smaller Tb^{3+} ion (0.923 Å) doping confirms our speculation on the correlation between weak ferromagnetism and oxygen distortion. A low field of 1 G is again used to minimize the $\text{Gd}^{3+}/\text{Tb}^{3+}$ contribution. Large WF contribution of magnetized moment of 1 – $7 \times 10^{-3} \mu_B/\text{Cu}^{2+}$ is observed below $T_N(\text{Cu})$ 282 K for $x=0$ and 276 K for $x=0.1$ and 0.5. Spin-reorientation temperature $T_{\text{sr}}(\text{Cu})$ remains around 22 K for all compounds. The rare earth $R(\text{Gd}/\text{Tb})$ sublattice orders antiferromagnetically at $T_N(R)$ of 6.2 K for $x=0.1$ and 0.5.

In conclusion, detailed Rietveld refinement gives a direct correlation between the oxygen distortion angle $\alpha(\text{Cu-O-Cu})$ and the ionic size in the $(\text{Gd}, M)_2\text{CuO}_4$ cuprates. For smaller (Gd, M) ions, tetragonal T' phase is no longer stable at room temperature and lattice layer mismatch lowers the symmetry to an orthorhombic O' phase. Weak ferromagnetic or canted antiferromagnetic (WF/CAF) ordering below $T_N(\text{Cu})$ is the direct result of this oxygen distortion angle that causes a non- 180° Cu-O-Cu coupling. True antiferromagnetic ordering was restored only at temperature below $T_{\text{sr}}(\text{Cu})$.

ACKNOWLEDGMENTS

This work was supported by the National Science Council of R.O.C. under contract Nos. NSC88-2112-M007-003 and NSC88-2112-M007-033. We thank Professor H.-C. I. Kao of the Tamkang University for titration measurements.

- ¹K. A. Kubat-Martin, Z. Fisk, and R. R. Ryan, *Acta Crystallogr., Sect. C: Cryst. Struct. Commun.* **44**, 1518 (1988), and references cited therein.
- ²J. D. Thompson, S.-W. Cheong, S. E. Brown, Z. Fisk, S. B. Oseroff, M. Tovar, D. C. Vier, and S. Schultz, *Phys. Rev. B* **39**, 6660 (1989).
- ³C. L. Seaman, N. Y. Ayoub, T. Bjornholm, E. A. Early, S. Ghamaty, B. W. Lee, J. T. Markert, J. J. Neumeier, P. K. Tsai, and M. B. Maple, *Physica C* **159**, 391 (1989).
- ⁴G. Xiao, M. Z. Cieplak, and C. L. Chien, *Phys. Rev. B* **40**, 4538 (1989).
- ⁵S. B. Oseroff, D. Rao, F. Wright, D. C. Vier, S. Schultz, J. D. Thompson, Z. Fisk, S.-W. Cheong, M. F. Hundley, and M. Tovar, *Phys. Rev. B* **41**, 1934 (1990).
- ⁶T. Chattopadhyay, P. J. Brown, B. Roessli, A. A. Stepanov, S. N. Barilo, and D. I. Zhigunov, *Phys. Rev. B* **46**, 5731 (1992).
- ⁷G. H. Hwang, J. H. Shieh, J. C. Ho, and H. C. Ku, *Physica C* **201**, 171 (1992).
- ⁸G. H. Hwang, J. H. Shieh, H. C. Ku, and J. C. Ho, *Chin. J. Phys. (Taipei)* **30**, 351 (1992).
- ⁹P. Adelman, R. Ahrens, G. Czjzek, G. Roth, H. Schmidt, and C. Steinleitner, *Phys. Rev. B* **46**, 3619 (1992).
- ¹⁰L. B. Steren, M. Tovar, and S. B. Oseroff, *Phys. Rev. B* **46**, 2874 (1992).
- ¹¹A. A. Stepanov, P. Wyder, T. Chattopadhyay, P. J. Brown, G. Fillion, I. M. Vitebsky, A. Deville, B. Gaillard, S. N. Barilo, and D. I. Zhigunov, *Phys. Rev. B* **48**, 12 979 (1993).
- ¹²M. Braden, W. Paulus, A. Cousson, P. Vigoureux, G. Heger, A. Goukassov, P. Bourges, and D. Petitgrand, *Europhys. Lett.* **25**, 625 (1994).
- ¹³A. Butera, M. Tovar, S. B. Oseroff, and Z. Fisk, *Phys. Rev. B* **52**, 13 444 (1995).
- ¹⁴H. C. Ku, H. M. Luo, Y. Y. Hsu, M. M. Sarker, and T. J. Lee, *J. Appl. Phys.* **85**, 5362 (1999).
- ¹⁵T. Chattopadhyay, P. J. Brown, and B. Roessli, *J. Appl. Phys.* **75**, 6816 (1994).
- ¹⁶H. Okada, M. Takano, and Y. Takeda, *Phys. Rev. B* **42**, 6813 (1990).
- ¹⁷M. Tovar, X. Obradors, F. Pérez, S. B. Oseroff, R. J. Duro, J. Rivas, D. Chateigner, P. Bordet, and J. Chenavas, *Phys. Rev. B* **45**, 4729 (1992).
- ¹⁸H. D. Yang, T. H. Meen, and Y. C. Chen, *Phys. Rev. B* **48**, 7720 (1993).
- ¹⁹T. Schultz, R. Smith, A. Fondado, C. Maley, T. Beacom, P. Tinklenberg, J. Gross, C. Saylor, S. B. Oseroff, Z. Fisk, S. W. Cheong, and T. E. Jones, *J. Appl. Phys.* **75**, 6723 (1994).
- ²⁰M. Braden, P. Adelman, P. Schweiss, and T. Woisczyk, *Phys. Rev. B* **53**, R2975 (1996).
- ²¹A. Butera, M. Tovar, S. B. Oseroff, and Z. Fisk, *Physica B* **233**, 241 (1997).
- ²²RIQAS program, Materials Data, Inc., Livermore, CA (1996).
- ²³*Handbook of Chemistry and Physics*, F-213, edited by R. C. Weast, 57th ed. (CRC Press, Cleveland, OH, 1976).
- ²⁴R. J. Birgeneau and G. Shirane, in *Physical Properties of High Temperature Superconductors I*, edited by D. M. Ginsburg (World Scientific, Singapore, 1989), Chap. 4.